

# NONLINEAR DIFFUSION PDES

*Erkut Erdem\**

*Hacettepe University*

*March 5<sup>th</sup>, 2012*

## CONTENTS

1	Perona-Malik Type Nonlinear Diffusion	1
2	Edge Enhancing Diffusion	5
	References	7

## 1 PERONA-MALIK TYPE NONLINEAR DIFFUSION

The main theory behind nonlinear diffusion models is to use nonlinear PDEs to create a scale space representation that consists of gradually simplified images where some image features such as edges are maintained or even enhanced. The earliest nonlinear diffusion model proposed in image processing is the so-called *anisotropic diffusion*<sup>1</sup> by Perona and Malik [2].

In their formulation, they replaced the constant diffusion coefficient of linear equation by a smooth nonincreasing diffusivity function  $g$  with  $g(0) = 1$ ,  $g(s) \geq 0$ , and  $\lim_{s \rightarrow \infty} g(s) = 0$ . As a consequence, the diffusivities become variable in both space and time. The Perona-Malik equation is

$$(1) \quad \frac{\partial u}{\partial t} = \nabla \cdot (g(|\nabla u|) \nabla u)$$

with homogeneous Neumann boundary conditions and the initial condition  $u^0(x) = f(x)$ ,  $f$  denoting the input image.

Perona and Malik suggested two different choices for the diffusivity function:

$$(2) \quad g(s) = \frac{1}{1 + s^2/\lambda^2},$$

$$(3) \quad g(s) = e^{-\frac{s^2}{\lambda^2}}$$

---

\*erkut@cs.hacettepe.edu.tr

<sup>1</sup>In fact, Perona-Malik equation is an isotropic nonhomogeneous equation as it uses a scalar-valued diffusivity. A true example of anisotropic diffusion model, edge-enhancing diffusion [3], will be summarized in Section 2.

where  $\lambda$  corresponds to a contrast parameter. These functions share similar characteristics, and result in similar effects on the diffusivities.

We review the 1D physical analysis of the Perona-Malik diffusion below since it clearly demonstrates the role of the contrast parameter  $\lambda$  and the main behavior of the equation [4]. For 1D case, the Perona-Malik equation is as follows:

$$(4) \quad \frac{\partial u}{\partial t} = \frac{\partial}{\partial x} \underbrace{(g(|u_x|)u_x)}_{\Phi(u_x)} = \Phi'(u_x)u_{xx}$$

with  $g(|u_x|) = \frac{1}{1+|u_x|^2/\lambda^2}$  or  $g(|u_x|) = e^{-\frac{|u_x|^2}{\lambda^2}}$ .

Figure 1 shows the diffusivity functions and the corresponding flux functions for linear diffusion and Perona-Malik type nonlinear diffusion. One can easily observe that for linear diffusion the diffusivity is constant ( $g(s) = 1$ ), which results in a linearly increasing flux function. As a result, all points, including the discontinuities, are smoothed equally. For Perona-Malik, the diffusivity is variable and decreases as  $|u_x|$  increases. It is evident that the decay in diffusivity is particularly rapid after the contrast parameter  $\lambda$ . This leads to two different behaviors in the diffusion process. Since  $\frac{\partial u}{\partial t} = \Phi'(u_x)u_{xx}$ , for the points where  $|u_x| < \lambda$ ,  $\Phi'(u_x) > 0$  which corresponds to lost in the material. For the points where  $|u_x| > \lambda$ , on the contrary,  $\Phi'(u_x) < 0$  which generates an enhancement in the material. Hence, although the diffusivity is always nonnegative, one can observe both *forward* and *backward* diffusions during the smoothing process, and the contrast parameter  $\lambda$  separates the regions of forward diffusion from the regions of backward diffusion.

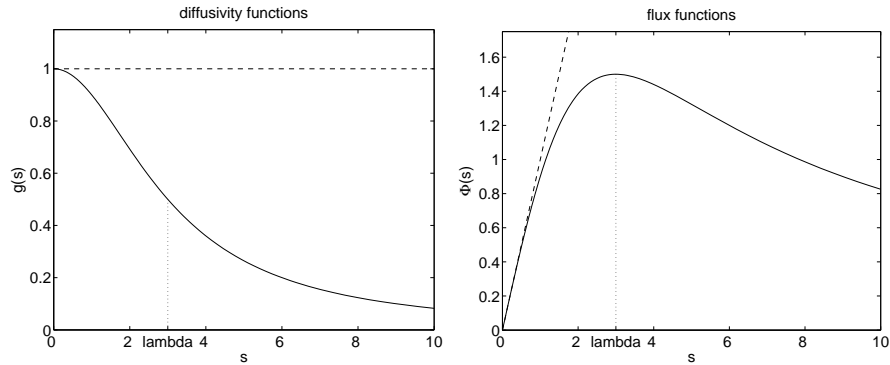


Figure 1: Diffusivities and the corresponding flux functions for linear diffusion (*plotted in dashed line*) and Perona-Malik type nonlinear diffusion (*plotted in solid line*). For Perona-Malik diffusivity  $g(s) = \frac{1}{1+s^2/\lambda^2}$  is used with  $\lambda = 3$ .

If we consider the 2D case, the diffusivities are reduced at the image locations where  $|\nabla u|^2$  is large. As  $|\nabla u|^2$  can be interpreted as a measure of edge likelihood, this means that the amount of smoothing is low along image edges. In particular, the contrast parameter  $\lambda$  specifies a measure that determines which edge points are to be preserved or blurred during the diffusion process. Even edges can be sharpened due to the local backward diffusion behavior as discussed for the 1D case. Since the backward



Figure 2: The staircasing effect. (a) Original noisy image. (b) Perona-Malik diffusion. (c) Regularized Perona-Malik diffusion.

diffusion is a well-known ill-posed process, this may cause an instability, the so-called *staircasing effect*, where a piece-wise smooth region in the original image evolves into many unintuitive piecewise constant regions. Figure 2 shows an example where this instability occurs. The unintuitive regions such as the one at the woman's face and shoulder are clearly visible in Figure 2(b). A possible solution to this drawback is to use regularized gradients in diffusivity computations [1] (Figure 2(c)).

Replacing the diffusivities  $g(|\nabla u|)$  with the regularized ones  $g(|\nabla u_\sigma|)$  leads to the following equation:

$$(5) \quad \frac{\partial u}{\partial t} = \nabla \cdot (g(|\nabla u_\sigma|) \nabla u)$$

where  $u_\sigma = G_\sigma * u$  represents a Gaussian-smoothed version of the image. Taking the equivalence of the Gaussian smoothing and the linear scale space into account,  $\nabla u_\sigma$  can also be considered as the gradient computed at a specific scale  $\sigma > 0$ .

Some example results of regularized Perona-Malik filtering with different diffusion times are shown in Figure 3 and Figure 4. It is evident from these images that the corresponding smoothing process diminishes noise while retaining or even enhancing edges since it considers a kind of a priori edge knowledge.

### Numerical Implementation

For numerical implementation, we use central differences to approximate the gradient magnitude at a pixel  $(i, j)$  in the diffusivity estimation,  $g_{i,j} = g(|\nabla u_{i,j}|)$ :

$$(6) \quad |\nabla u_{i,j}| = \sqrt{\left(\frac{du_{i,j}}{dx}\right)^2 + \left(\frac{du_{i,j}}{dy}\right)^2} \approx \sqrt{\left(\frac{u_{i+1,j} - u_{i-1,j}}{2}\right)^2 + \left(\frac{u_{i,j+1} - u_{i,j-1}}{2}\right)^2}.$$

The Perona-Malik equation (Equation 1) is first discretized w.r.t. spatial variables.

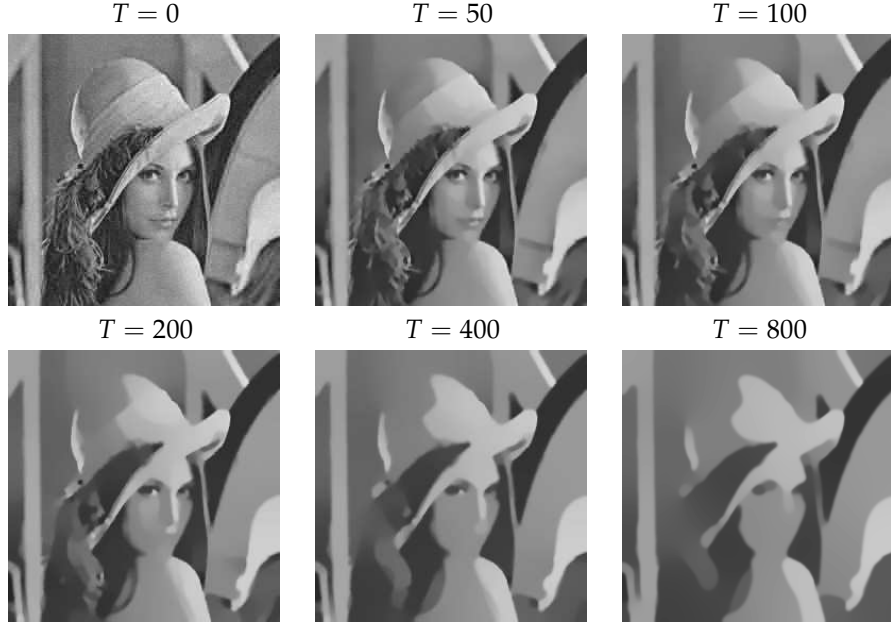


Figure 3: Reg. Perona-Malik results for different diffusion time ( $\lambda = 1, \sigma = 1$ ).

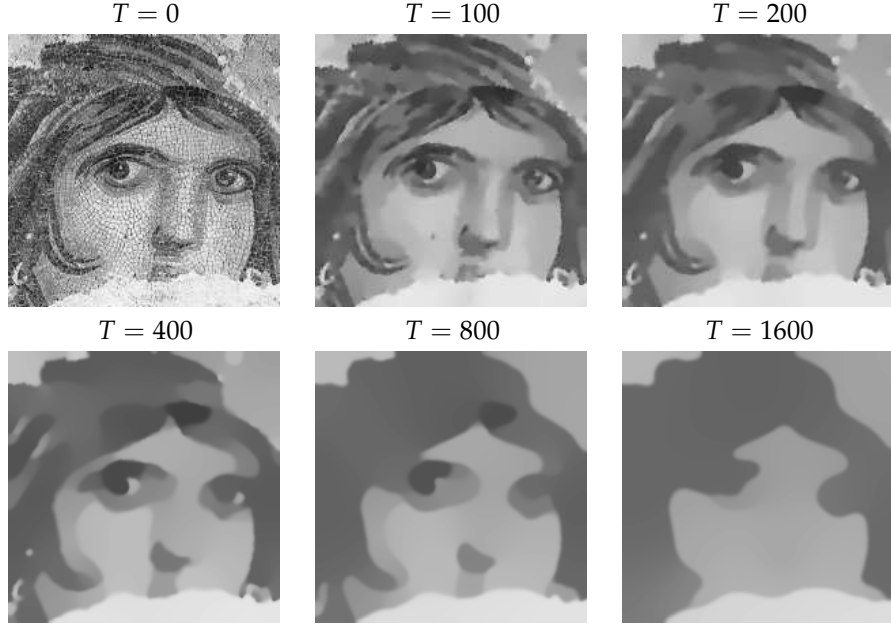


Figure 4: Reg. Perona-Malik results for different diffusion times ( $\lambda = 1, \sigma = 1$ ).

This results in the following space-discrete equation:

$$\begin{aligned}
 \frac{\partial u}{\partial t} &= \frac{\partial}{\partial x} (g(|\nabla u|)u_x) + \frac{\partial}{\partial y} (g(|\nabla u|)u_y), \\
 \text{(7)} \quad \frac{du_{i,j}}{dt} &= g_{i+\frac{1}{2},j} \cdot (u_{i+1,j} - u_{i,j}) - g_{i-\frac{1}{2},j} \cdot (u_{i,j} - u_{i-1,j}) \\
 &+ g_{i,j+\frac{1}{2}} \cdot (u_{i,j+1} - u_{i,j}) - g_{i,j-\frac{1}{2}} \cdot (u_{i,j} - u_{i,j-1}).
 \end{aligned}$$

---

$u_{i-1,j-1}$	$u_{i,j-1}$	$u_{i+1,j-1}$
	$g_{i,j-\frac{1}{2}}$	
$u_{i-1,j}$	$g_{i+\frac{1}{2},j}$	$u_{i,j}$
	$g_{i+\frac{1}{2},j}$	$g_{i+\frac{1}{2},j}$
$u_{i-1,j+1}$	$u_{i,j+1}$	$u_{i+1,j+1}$

Figure 5: Discretization grid used in (Equation 7).

This discretization scheme requires the diffusivities to be estimated at mid-pixel points (Figure 5). They are simply computed by taking averages of the diffusivities over neighboring pixels:

$$(8) \quad g_{i\pm\frac{1}{2},j} = \frac{g_{i\pm 1,j} + g_{i,j}}{2}, \quad g_{i,j\pm\frac{1}{2}} = \frac{g_{i,j\pm 1} + g_{i,j}}{2}.$$

The time derivative in (Equation 7) can be discretized using forward difference. This yields an iterative scheme with an explicit time discretization, where homogeneous Neumann boundary condition is imposed along the image boundary

$$(9) \quad \frac{u_{i,j}^{k+1} - u_{i,j}^k}{\Delta t} = g_{i+\frac{1}{2},j}^k \cdot u_{i+1,j}^k + g_{i-\frac{1}{2},j}^k \cdot u_{i-1,j}^k + g_{i,j+\frac{1}{2}}^k \cdot u_{i,j+1}^k + g_{i,j-\frac{1}{2}}^k \cdot u_{i,j-1}^k - \left( g_{i+\frac{1}{2},j}^k + g_{i-\frac{1}{2},j}^k + g_{i,j+\frac{1}{2}}^k + g_{i,j-\frac{1}{2}}^k \right) \cdot u_{i,j}^k$$

with  $\Delta t$  denoting the time step. For the Perona-Malik diffusion, the stability requirement is again  $\Delta t \leq 0.25$ .

## 2 EDGE ENHANCING DIFFUSION

The nonlinear diffusion model proposed by Perona and Malik employs a scalar-valued diffusivity function to guide the smoothing process as summarized in Section 1. The diffusivities are reduced at the image locations where the magnitude of image gradient  $|\nabla u|^2$  is large, and as a result, the edges are preserved or even enhanced. In [3], Weickert suggested an alternative approach that additionally takes direction of the image gradients into account. The suggested model is an anisotropic nonlinear diffusion model with better edge enhancing capabilities.

In general, any anisotropic nonlinear diffusion can be described by the equation

$$(10) \quad \frac{\partial u}{\partial t} = \nabla \cdot (D(\nabla u) \nabla u)$$

where  $u$  is the smoothed image that is initialized with the input image  $f$  (that is  $u^0(x) = f(x)$ ), and  $D$  represents a matrix-valued diffusion tensor that describes the

smoothing directions and the corresponding diffusivities. One can easily observe that for linear diffusion the diffusion tensor can be defined as  $D(\nabla u) = I$ , which results in a constant diffusion coefficient for all image points in all directions. Similarly, for Perona-Malik type nonlinear diffusion,  $D(\nabla u) = g(|\nabla u_\sigma|)I$ . Such a choice reduces the amount of smoothing at image edges, but in an equal amount in all directions. In actual anisotropic setting, the diffusion tensor  $D$  is defined as a function of the structure tensor given by

$$(11) \quad J(\nabla u) = \nabla u \nabla u^T = \begin{bmatrix} u_x^2 & u_x u_y \\ u_x u_y & u_y^2 \end{bmatrix}.$$

The structure tensor  $J(\nabla u)$  can be interpreted as an image feature describing the local orientation information. It has an orthonormal basis of eigenvectors  $v_1$  and  $v_2$  with  $v_1 \parallel \nabla u$  and  $v_2 \perp \nabla u$ , and the corresponding eigenvalues  $\lambda_1 = |\nabla u|^2$  and  $\lambda_2 = 0$ . It is important to note that noise significantly affects the tensor estimation. Thus the given image  $u$  is usually convolved with a Gaussian kernel  $G_\sigma$  with a relatively small standard deviation  $\sigma$  as a presmoothing step and the structure tensor is computed accordingly by using  $\nabla u_\sigma = \nabla(G_\sigma * u)$  instead of  $\nabla u$ .

The main idea behind edge enhancing diffusion is to use the structure tensor as an image/edge descriptor to construct a diffusion tensor that reduces the amount of smoothing across the edges while smoothing is still carried out along the edges. In order to perform this, Weickert proposed to utilize same orthonormal basis of eigenvectors  $v_1 \parallel \nabla u_\sigma$  and  $v_2 \perp \nabla u_\sigma$  estimated from the structure tensor  $J(\nabla u_\sigma)$  with the following choice of eigenvalues satisfying  $\frac{\lambda_1(|\nabla u_\sigma|)}{\lambda_2(|\nabla u_\sigma|)} \rightarrow 0$  for  $|\nabla u_\sigma| \rightarrow \infty$

$$(12) \quad \lambda_1(|\nabla u_\sigma|) = \begin{cases} 1 & \text{if } |\nabla u_\sigma| = 0 \\ 1 - \exp\left(-\frac{3.31488}{(|\nabla u_\sigma|/\lambda)^8}\right) & \text{otherwise,} \end{cases}$$

$$(13) \quad \lambda_2(|\nabla u_\sigma|) = 1$$

where  $\lambda$  denotes the contrast parameter.

Such a choice preserves and enhances image edges by reducing the diffusivity  $\lambda_1$  perpendicular to edges for sufficiently large values of  $|\nabla u_\sigma|$ . Specifically, the diffusion tensor is given by the formula

$$(14) \quad D = \begin{bmatrix} (u_\sigma)_x & -(u_\sigma)_y \\ (u_\sigma)_y & (u_\sigma)_x \end{bmatrix} \cdot \begin{bmatrix} \lambda_1(|\nabla u_\sigma|) & 0 \\ 0 & \lambda_2(|\nabla u_\sigma|) \end{bmatrix} \cdot \begin{bmatrix} (u_\sigma)_x & -(u_\sigma)_y \\ (u_\sigma)_y & (u_\sigma)_x \end{bmatrix}^{-1}.$$

Figure 6 and Figure 7 illustrate example results of edge enhancing diffusion filter for different diffusion times. As it can be clearly seen from these images, the corresponding smoothing process diminishes noise and fine image details while retaining and even enhancing edges as in the Perona-Malik type nonlinear diffusion. On the other hand, the corners become more rounded in the anisotropic model compared to the Perona-Malik filter (cf. Figure 3 and Figure 4) since edge enhancing diffusion allows smoothing along edges while preventing smoothing across them. As discussed in [4], this causes a slight shrinking effect in the image structures, which eliminates

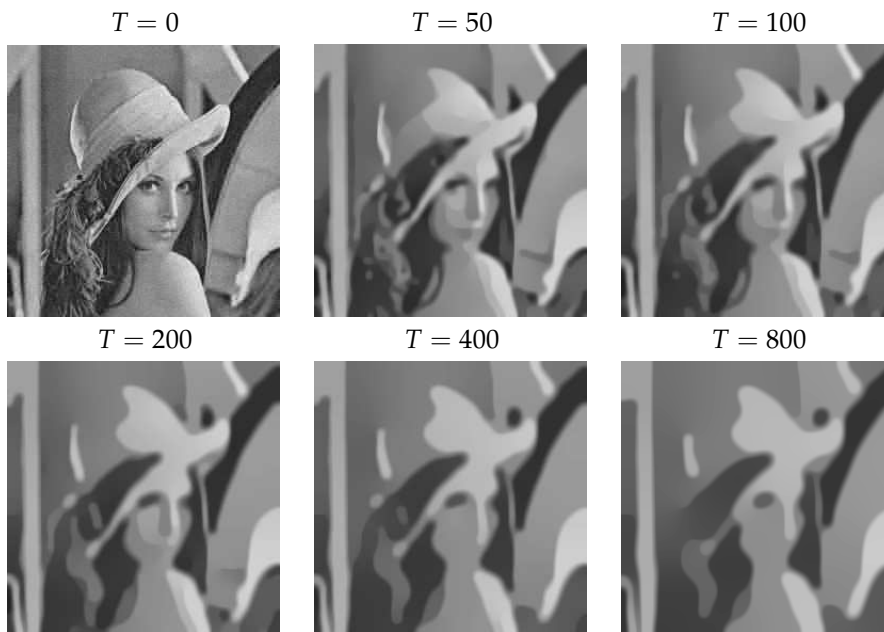


Figure 6: Edge enhancing diffusion results for different diffusion times ( $\lambda = 2, \sigma = 1$ ).

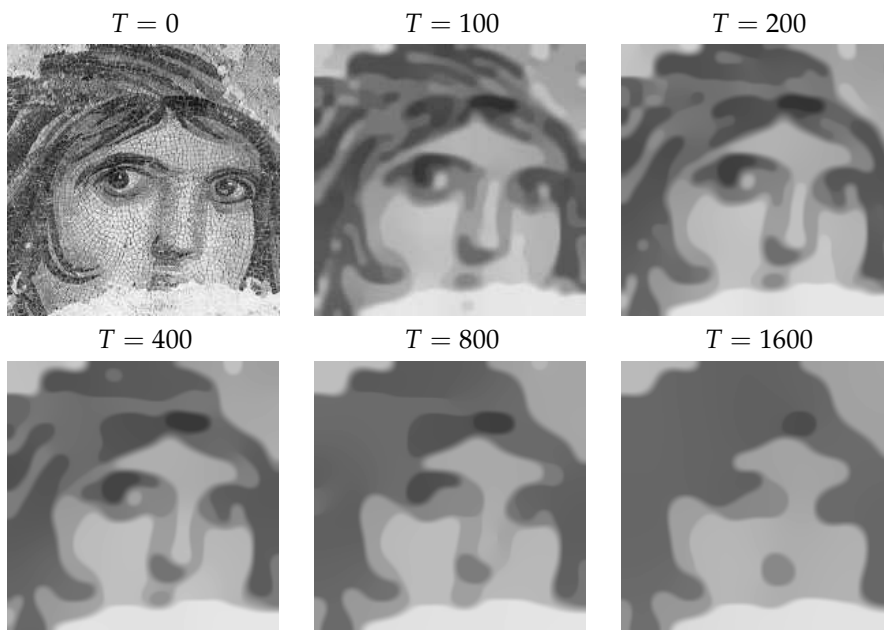


Figure 7: Edge enhancing diffusion results for different diffusion times ( $\lambda = 1.8, \sigma = 1$ ).

fine or thin structures better than the Perona-Malik model. Thus, through this process one can capture semantically more correct image regions.

REFERENCES

- [1] F. Catté, P.-L. Lions, J.-M. Morel, and T. Coll. Image selective smoothing and edge detection by nonlinear diffusion. *SIAM J. Numer. Anal.*, 29(1):182–193, 1992.
- [2] P. Perona and J. Malik. Scale-space and edge detection using anisotropic diffusion. *IEEE Trans. Pattern Anal. Mach. Intell.*, 12:629–639, 1990.
- [3] J. Weickert. Anisotropic diffusion filters for image processing based quality control. In *Proc. Seventh European Conference on Mathematics in Industry*, pages 355–362, 1994.
- [4] J. Weickert. *Anisotropic Diffusion in Image Processing*. Teubner, Stuttgart, 1998.